frontiers in Oncology

OPINION
published: 11 March 2016
doi: 10.3389/fonc.2016.00059

Potential Clinical Roles for Metabolic Imaging with Hyperpolarized [1-^{13}C]Pyruvate

*Eva M. Serrao[1,2] and Kevin M. Brindle[1,2]**

[1] Li Ka Shing Centre, Cancer Research UK Cambridge Institute, University of Cambridge, Cambridge, UK, [2] Department of Biochemistry, University of Cambridge, Cambridge, UK

Keywords: cancer, metabolism, imaging, hyperpolarized, pyruvate, therapy monitoring

Clinical oncology relies increasingly on biomedical imaging, with anatomical imaging, especially using CT and ^{1}H-MRI, forming the mainstay of patient assessment, from diagnosis to treatment monitoring. However, the need for further improvements in specificity and sensitivity, coupled with imaging techniques that are reaching their limit of clinically attainable spatial resolution, has resulted in the emergence and growing use of imaging techniques with additional functional readouts, such as ^{18}FDG-PET and multiparametric MRI. These techniques add a new dimension to our understanding of the biological behavior of tumors, allowing a more personalized approach to patient management.

An important functional imaging target in cancer is metabolism. PET measurements of ^{18}Fluorodeoxyglucose uptake (^{18}FDG-PET), a ^{18}F-labeled glucose analog, and ^{1}H-MRS measurements, have both been used to investigate tumor metabolism for diagnostic purposes. However, clinical applications of MRS have been hampered by low sensitivity and consequently low spatial and temporal resolution (1). Nuclear spin hyperpolarization of ^{13}C-labeled substrates, using dynamic nuclear polarization (DNP), which radically increases the sensitivity of these substrates to detection by ^{13}C MRS (2), has created a renewed interest in MRS measurements of tissue metabolism. Successful translation of this technique to the clinic was achieved recently with measurements of [1-^{13}C]pyruvate metabolism in prostate cancer (3) (see **Figure 1**). We explore here the potential clinical roles for metabolic imaging with hyperpolarized [1-^{13}C]pyruvate.

OPEN ACCESS

Edited by:
Franca Podo,
Istituto Superiore di Sanitá, Italy

Reviewed by:
Natalie Julie Serkova,
University of Colorado, USA
Sarah Nelson,
University of California San Francisco, USA

****Correspondence:***
Kevin M. Brindle
kmb1001@cam.ac.uk

Specialty section:
This article was submitted to Cancer Imaging and Diagnosis, a section of the journal Frontiers in Oncology

Received: *23 December 2015*
Accepted: *28 February 2016*
Published: *11 March 2016*

Citation:
Serrao EM and Brindle KM (2016) Potential Clinical Roles for Metabolic Imaging with Hyperpolarized [1-^{13}C]Pyruvate. Front. Oncol. 6:59. doi: 10.3389/fonc.2016.00059

DYNAMIC NUCLEAR POLARIZATION

Dynamic nuclear polarization, which can increase the signal-to-noise ratio in the solution-state ^{13}C MR experiment by 10^{4}- to 10^{5}-fold (4), has enabled *in vivo* imaging of various metabolites and their enzymatic conversion into other species, as well as metabolic fluxes in central metabolic pathways, such as glycolysis (5–7) and the tricarboxylic acid cycle (8–10). The principle limitation of the technique is the short half-life of the polarization; for [1-^{13}C]pyruvate *in vivo*, this is typically between 30 and 40 s, which means that the hyperpolarized signal will last for 2–3 min. Therefore, the substrate, whose metabolism is to be imaged, must be transferred promptly from the polarizer, injected intravenously, and then transit quickly *via* the circulation to the tissue of interest, where it should be taken up and metabolized rapidly (11, 12). To date, numerous molecules, in addition to ^{13}C-labeled pyruvate, have been successfully hyperpolarized and their metabolism imaged, including [1,4-$^{13}C_2$]fumarate, as a marker of cell necrosis (13, 14); [U-^{2}H,

Abbreviations: ^{18}FDG, ^{18}Fluorodeoxyglucose; MRS, magnetic resonance spectroscopy; MRSI, magnetic resonance spectroscopic imaging; PET, positron emission tomography.

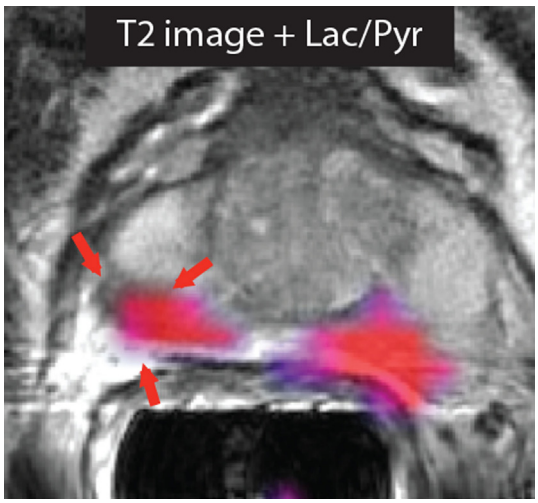

FIGURE 1 | Imaging prostate cancer with hyperpolarized [1-^{13}C]pyruvate. The T_2-weighted image of a patient with biopsy-proven bilateral prostate cancer showed only a unilateral decrease in signal intensity. However, the metabolic image ([1-^{13}C]lactate/[1-^{13}C]pyruvate ratio) detected disease on both the right and left sides of the prostate. Reproduced from Nelson et al. (3) with permission.

U-^{13}C]glucose for assessment of glycolytic and pentose phosphate pathway activities and for detecting early treatment response (7); ^{13}C-labeled bicarbonate for *in vivo* mapping of pH (15); and ^{13}C-labeled urea as a marker of perfusion (16), among others (13, 16–18). Despite initial interest in vascular imaging (19–21), the main focus has been on imaging metabolism in tumors (13, 17, 22) and cardiac tissue (23–27).

PYRUVATE

Pyruvate is an important intermediate in many biochemical pathways (28). As an end product of glycolysis, pyruvate can be reduced by NADH to generate lactate, in the readily reversible reaction catalyzed by lactate dehydrogenase, or transaminated by glutamate, in the reversible reaction catalyzed by alanine aminotransferase (ALT), to form alanine. In tissues with high levels of mitochondrial activity, such as heart muscle, pyruvate may be irreversibly decarboxylated to form carbon dioxide in the reaction catalyzed by the mitochondrial pyruvate dehydrogenase (PDH) complex (26). Since increased aerobic glycolysis is a well-recognized hallmark of cancer (29, 30), this has made it an attractive pathway to probe for diagnostic and treatment monitoring purposes (3, 17, 31).

Potential Clinical Roles

Preclinical studies have demonstrated that hyperpolarized [1-^{13}C]pyruvate is a promising probe for oncological imaging, with increased lactate labeling observed in tumors as compared to normal tissues (31, 32). The substrate has the potential to be used in many steps of patient management. A recent study demonstrated the potential of hyperpolarized [1-^{13}C]pyruvate as an imaging biomarker for early detection and secondary screening of pancreatic cancer, where a decrease in the hyperpolarized [1-^{13}C]alanine/[1-^{13}C]lactate ratio was observed in the progression from precursor lesions to adenocarcinoma (33). In another study, [1-^{13}C]pyruvate detected metabolic changes prior to tumor formation (34). Additionally, in the first reported clinical trial in prostate cancer, increased lactate labeling was observed in histologically confirmed areas of disease that were not identifiable by conventional ^{1}H-MRI measurements (3) (**Figure 1**). The few studies that have explored the role of [1-^{13}C]pyruvate in grading and prognosis, which were in the transgenic mouse model of prostate adenocarcinoma (TRAMP), have also produced promising results (35, 36). Tumor grading by biopsy can sometimes be difficult depending on the accessibility of the organ of interest. Translation of the DNP technique to the clinic may allow more accurate targeting of biopsy procedures. Since lactate labeling is increased in regions of hypoxia, the technique also has the potential to be used for treatment planning in radiotherapy (37, 38). Clinical assessments of tumor responses to treatment are still based largely on observed changes in tumor size (39). However, this might not always be appropriate, particularly for detection of early responses or if the drug does not result in tumor shrinkage, for example, in the case of antiangiogenic drugs (40, 41). Additionally, treatment assessment using ^{18}FDG-PET is difficult in some organs, e.g., prostate and brain, due to both low tumor uptake and increased background uptake, respectively (40). Evaluation of treatment response is likely to be the clinical scenario where hyperpolarized [1-^{13}C]pyruvate will have the most impact, as it could lead to immediate changes in clinical management, allowing the clinician to change a non-responding patient to a more effective drug at an early stage (40). Early assessment of treatment response could also be used to accelerate the introduction of new drugs into the clinic by providing an indication of drug efficacy in early stage clinical trials. In support of this are numerous studies showing early decreases in hyperpolarized ^{13}C-labeled exchange between injected [1-^{13}C]pyruvate and the endogenous lactate pool in a range of cancer models following treatment with cytotoxic chemotherapy (17, 42), targeted drugs (43–45), and radiotherapy (41, 46, 47).

There is as yet no direct evidence to support the suggestion that residual disease/recurrence can be identified by increased lactate labeling. However, observations of increased lactate labeling in areas of disease and following disease progression (3, 33) make this likely. There is, however, evidence that hyperpolarized [1-^{13}C]pyruvate can be used to assess normal tissue toxicity, with an increase in the [1-^{13}C]lactate/[1-^{13}C]pyruvate ratio occurring in radiation-induced lung injury (48, 49).

ADVANTAGES OF METABOLIC IMAGING WITH [1-^{13}C]PYRUVATE

Advantages Compared to ^{18}FDG-PET

Metabolic imaging of cancer in the clinic has principally been with ^{18}FDG-PET, which has been used to stage tumors

and to assess treatment response. Despite its high sensitivity and capability to provide whole-body images, the use of ionizing radiation is a drawback, limiting its application in children and women of reproductive age, and when multiple investigations are needed, for example, as might be required for guiding treatment in an individual patient. A similar clinical role can be envisaged for [1-^{13}C]pyruvate as has been established for ^{18}FDG-PET. Both techniques can be used to detect increased glycolytic flux (50) and have been shown to be comparably sensitive in detecting tumor response to treatment (51). However, since hyperpolarized [1-^{13}C]pyruvate effectively detects lactate accumulation (11), a defining feature of cancer metabolism, i.e., the failure to oxidize pyruvate in the presence of oxygen and reduce it instead to lactate (the "Warburg Effect"), this means that hyperpolarized [1-^{13}C]pyruvate may be more specific for detecting cancer than ^{18}FDG-PET. The latter detects only elevated levels of glucose uptake, which is a feature of many normal tissues and cancer, for example, the brain. The specificity of cancer detection by hyperpolarized [1-^{13}C]pyruvate may be confounded, however, by the presence of hypoxia, which will also lead to lactate accumulation and increased lactate labeling (38). Another drawback of imaging with hyperpolarized [1-^{13}C]pyruvate is that the short half-life of the polarization precludes whole-body imaging.

Advantages Compared to ^{1}H MRS

^{1}H-MR spectroscopy and spectroscopic imaging measurements of tissue metabolite profiles are label-free and have found some applications, for example, in identifying different types of brain tumor (52). A notable example is the detection of 2-hydroxyglutarate, which can be used to identify glioblastomas with isocitrate dehydrogenase mutations (IDH) (53). ^{1}H MRSI has also proved to be important in the prostate, where it can improve the specificity of detection and determination of tumor extent when combined with other MR imaging sequences (54). However, detectable metabolites are present in only millimolar concentrations, as compared to tissue water protons, which are present at ~80M, which results in long data acquisition times and limited spatial resolution. In addition, data processing can be more complex and the biochemical information provided may be unfamiliar to many clinicians, which has limited routine clinical application. Moreover, ^{1}H MR spectroscopy and spectroscopic images of metabolite profiles provide a static picture of tumor metabolism. On the other hand, imaging with hyperpolarized ^{13}C-labeled substrates provides dynamic metabolic flux information in the form of images that can be acquired at relatively high spatial and temporal resolutions and therefore should provide an improved assessment of tumor behavior. Additionally, coinjection of different hyperpolarized substrates could also provide additional functional information in the same acquisition, e.g., pyruvate for assessing glycolytic activity and urea for assessing tumor perfusion (55).

COMBINING METABOLIC IMAGING WITH HYPERPOLARIZED [1-^{13}C]PYRUVATE WITH NEW TECHNOLOGIES

PET-MRI

This is an emerging combined imaging modality with significant potential for clinical assessment of cancer patients (56). Simultaneous PET-MR measurements with hyperpolarized ^{13}C- and ^{18}F-labeled substrates would allow a multiparametric assessment of the primary lesion and its metastases in a single imaging session, which potentially could be used to identify imaging-based phenotypes that have prognostic value and which may give a more specific readout of treatment response. For example, PET measurements of ^{18}FDG uptake assess just the first three steps in tumor glucose metabolism, i.e., delivery *via* the bloodstream, uptake on the glucose transporters, and phosphorylation and trapping in the reaction catalyzed by hexokinase. ^{13}C MRSI measurements of the exchange of hyperpolarized ^{13}C-labeled exchange between injected [1-^{13}C]pyruvate and the endogenous lactate pool again assess delivery *via* the bloodstream and effectively the last two steps in the glycolytic pathway, i.e., the steps catalyzed by lactate dehydrogenase and the plasma membrane monocarboxylate transporters. Therefore, by combining ^{18}FDG-PET and hyperpolarized [1-^{13}C]pyruvate measurements, we may be able to assess flux in the entire glycolytic pathway, for example, increased mitochondrial oxidation of pyruvate may have no effect on ^{18}FDG uptake but could decrease ^{13}C labeling of lactate. There are other PET probes of tumor metabolism that could also be used alongside hyperpolarized [1-^{13}C]pyruvate, and which could provide complementary information. These include ^{11}C-acetate, as a marker of fatty acid synthesis, and labeled glutamine, which can be used to assess glutaminolysis; both of which are upregulated in tumor cells (57, 58). These PET probes may be especially useful in tumors where ^{18}FDG is ineffective, e.g., in prostate tumors (59) and in gliomas (60), and where the corresponding hyperpolarized ^{13}C-labeled probes are limited. For example, the metabolism of hyperpolarized [1-^{13}C]acetate has been detected *in vivo* (61); however, the short lifetime of the hyperpolarization means that it could not be used to monitor fatty acid synthesis, where PET studies with [1-^{11}C]acetate in animal tumor models have shown that it can take over 60 min before there is substantial incorporation into the fatty acid pool (62). In the case of [5-^{13}C] glutamine, a relatively short hyperpolarization lifetime and slow metabolism (63) has precluded imaging *in vivo* (64).

Liquid Biopsies

Blood and urine biomarkers, obtained from "liquid biopsies," are also evolving, providing information in a non-invasive way allied to the advantages of collection simplicity and relatively low cost. Many body fluid biomarkers have been reported for different types of cancer; however, few have become established in the clinic, usually because they lack specificity. A recent promising example is a panel of three urine biomarkers for early detection of pancreatic cancer (65). Rapid advances in DNA sequencing technology have allowed somatic mutations present in tumor cells to

be detected and tracked in blood-borne circulating tumor DNA (ctDNA). These fragments of DNA, which have been detected with most types of cancer, have been demonstrated to have potential roles in early detection, staging, and in detecting response to therapy and acquired resistance to treatment (66, 67). Although measurements with hyperpolarized ^{13}C-labeled cell substrates and these new circulating biomarkers are still their infancy it seems likely that they will provide complementary information, for example, in the assessment of tumor heterogeneity.

CONCLUSION AND FUTURE DIRECTIONS

Imaging with hyperpolarized ^{13}C-labeled cell substrates has the potential to become a powerful tool in many steps of clinical evaluation, allowing a more personalized approach to treatment. The first clinical trial established the feasibility of imaging human tumors with hyperpolarized [1-^{13}C]pyruvate. Since this substrate can be used to assess glycolysis, which is upregulated in many tumors, then this should make it a very general tool for oncological imaging in the clinic. Despite the biological insights that imaging with hyperpolarized ^{13}C-labeled substrates promises to deliver in the clinic, it will nevertheless have to prove itself against established and emerging clinical techniques, demonstrating that it can provide unique information that changes clinical practice.

AUTHOR CONTRIBUTIONS

Both authors listed, have made substantial, direct, and intellectual contribution to the work, and approved it for publication.

ACKNOWLEDGMENTS

Work in KB's laboratory is supported by a Cancer Research UK Programme grant (17242) and the CRUK-EPSRC Imaging Centre in Cambridge and Manchester (16465). Clinical studies are funded by a Strategic Award from the Wellcome Trust (095962). ES was a recipient of a fellowship from the European Union Seventh Framework Programme (FP7/2007-2013) under the Marie Curie Initial Training Network *METAFLUX* (project number 264780). ES also acknowledges the educational support of the Programme for Advanced Medical Education from Calouste Gulbenkian Foundation, Champalimaud Foundation, Ministerio de Saude, and Fundacao para a Ciencia e Tecnologia, Portugal.

REFERENCES

1. Glunde K, Bhujwalla ZM. Metabolic tumor imaging using magnetic resonance spectroscopy. *Semin Oncol* (2011) **38**:26–41.1. doi:10.1053/j.seminoncol.2010.11.001
2. Ardenkjaer-Larsen JH, Fridlund B, Gram A, Hansson G, Hansson L, Lerche MH, et al. Increase in signal-to-noise ratio of >10,000 times in liquid-state NMR. *Proc Natl Acad Sci U S A* (2003) **100**:10158–63. doi:10.1073/pnas.1733835100
3. Nelson SJ, Kurhanewicz J, Vigneron DB, Larson PE, Harzstark AL, Ferrone M, et al. Metabolic imaging of patients with prostate cancer using hyperpolarized [1-^{13}C]pyruvate. *Sci Transl Med* (2013) **5**:198ra108. doi:10.1126/scitranslmed.3006070
4. Brindle KM, Bohndiek SE, Gallagher FA, Kettunen MI. Tumor imaging using hyperpolarized ^{13}C magnetic resonance spectroscopy. *Magn Reson Med* (2011) **66**:505–19. doi:10.1002/mrm.22999
5. Meier S, Karlsson M, Jensen PR, Lerche MH, Duus JO. Metabolic pathway visualization in living yeast by DNP-NMR. *Mol Biosyst* (2011) **7**:2834–6. doi:10.1039/c1mb05202k
6. Harris T, Degani H, Frydman L. Hyperpolarized ^{13}C NMR studies of glucose metabolism in living breast cancer cell cultures. *NMR Biomed* (2013) **26**:1831–43. doi:10.1002/nbm.3024
7. Rodrigues TB, Serrao EM, Kennedy BW, Hu DE, Kettunen MI, Brindle KM. Magnetic resonance imaging of tumor glycolysis using hyperpolarized ^{13}C-labeled glucose. *Nat Med* (2014) **20**:93–7. doi:10.1038/nm.3416
8. Schroeder MA, Atherton HJ, Ball DR, Cole MA, Heather LC, Griffin JL, et al. Real-time assessment of Krebs cycle metabolism using hyperpolarized ^{13}C magnetic resonance spectroscopy. *FASEB J* (2009) **23**:2529–38. doi:10.1096/fj.09-129171
9. Merritt ME, Harrison C, Sherry AD, Malloy CR, Burgess SC. Flux through hepatic pyruvate carboxylase and phosphoenolpyruvate carboxykinase detected by hyperpolarized ^{13}C magnetic resonance. *Proc Natl Acad Sci U S A* (2011) **108**:19084–9. doi:10.1073/pnas.1111247108
10. Chen AP, Hurd RE, Schroeder MA, Lau AZ, Gu YP, Lam WW, et al. Simultaneous investigation of cardiac pyruvate dehydrogenase flux, Krebs cycle metabolism and pH, using hyperpolarized [1,2-^{13}C2]pyruvate in vivo. *NMR Biomed* (2012) **25**:305–11. doi:10.1002/nbm.1749
11. Gallagher FA, Bohndiek SE, Kettunen MI, Lewis DY, Soloviev D, Brindle KM. Hyperpolarized ^{13}C MRI and PET: *in vivo* tumor biochemistry. *J Nucl Med* (2011) **52**:1333–6. doi:10.2967/jnumed.110.085258
12. Brindle KM. Imaging metabolism with hyperpolarized ^{13}C-labeled cell substrates. *J Am Chem Soc* (2015) **137**:6418–27. doi:10.1021/jacs.5b03300
13. Gallagher FA, Kettunen MI, Hu DE, Jensen PR, Zandt RI, Karlsson M, et al. Production of hyperpolarized [1,4-$^{13}C_2$]malate from [1,4-$^{13}C_2$]fumarate is a marker of cell necrosis and treatment response in tumors. *Proc Natl Acad Sci U S A* (2009) **106**:19801–6. doi:10.1073/pnas.0911447106
14. Clatworthy MR, Kettunen MI, Hu DE, Mathews RJ, Witney TH, Kennedy BW, et al. Magnetic resonance imaging with hyperpolarized [1,4-^{13}C2]fumarate allows detection of early renal acute tubular necrosis. *Proc Natl Acad Sci U S A* (2012) **109**:13374–9. doi:10.1073/pnas.1205539109
15. Gallagher FA, Kettunen MI, Day SE, Hu DE, Ardenkjaer-Larsen JH, Zandt R, et al. Magnetic resonance imaging of pH *in vivo* using hyperpolarized ^{13}C-labelled bicarbonate. *Nature* (2008) **453**:940–3. doi:10.1038/nature07017
16. Wilson DM, Keshari KR, Larson PE, Chen AP, Hu S, Van Criekinge M, et al. Multi-compound polarization by DNP allows simultaneous assessment of multiple enzymatic activities *in vivo*. *J Magn Reson* (2010) **205**:141–7. doi:10.1016/j.jmr.2010.04.012
17. Day SE, Kettunen MI, Gallagher FA, Hu DE, Lerche M, Wolber J, et al. Detecting tumor response to treatment using hyperpolarized ^{13}C magnetic resonance imaging and spectroscopy. *Nat Med* (2007) **13**:1382–7. doi:10.1038/nm1650
18. Kurhanewicz J, Vigneron DB, Brindle K, Chekmenev EY, Comment A, Cunningham CH, et al. Analysis of cancer metabolism by imaging hyperpolarized nuclei: prospects for translation to clinical research. *Neoplasia* (2011) **13**:81–97. doi:10.1593/neo.101102
19. Golman K, Ardenkjaer-Larsen JH, Svensson J, Axelsson O, Hansson G, Hansson L, et al. ^{13}C-angiography. *Acad Radiol* (2002) **9**(Suppl 2):S507–10. doi:10.1016/S1076-6332(03)80278-7
20. Svensson J, Mansson S, Johansson E, Petersson JS, Olsson LE. Hyperpolarized ^{13}C MR angiography using trueFISP. *Magn Reson Med* (2003) **50**:256–62. doi:10.1002/mrm.10530
21. Mansson S, Johansson E, Magnusson P, Chai CM, Hansson G, Petersson JS, et al. ^{13}C imaging-a new diagnostic platform. *Eur Radiol* (2006) **16**:57–67. doi:10.1007/s00330-005-2806-x
22. Chen AP, Albers MJ, Cunningham CH, Kohler SJ, Yen YF, Hurd RE, et al. Hyperpolarized ^{13}C spectroscopic imaging of the TRAMP mouse at 3T-initial experience. *Magn Reson Med* (2007) **58**:1099–106. doi:10.1002/mrm.21256
23. Merritt ME, Harrison C, Storey C, Jeffrey FM, Sherry AD, Malloy CR. Hyperpolarized ^{13}C allows a direct measure of flux through a single

enzyme-catalyzed step by NMR. *Proc Natl Acad Sci U S A* (2007) **104**:19773–7. doi:10.1073/pnas.0706235104
24. Golman K, Petersson JS, Magnusson P, Johansson E, Akeson P, Chai CM, et al. Cardiac metabolism measured noninvasively by hyperpolarized ^{13}C MRI. *Magn Reson Med* (2008) **59**:1005–13. doi:10.1002/mrm.21460
25. Merritt ME, Harrison C, Storey C, Sherry AD, Malloy CR. Inhibition of carbohydrate oxidation during the first minute of reperfusion after brief ischemia: NMR detection of hyperpolarized $^{13}CO_2$ and $H^{13}CO_3$. *Magn Reson Med* (2008) **60**:1029–36. doi:10.1002/mrm.21760
26. Schroeder MA, Cochlin LE, Heather LC, Clarke K, Radda GK, Tyler DJ. *In vivo* assessment of pyruvate dehydrogenase flux in the heart using hyperpolarized carbon-13 magnetic resonance. *Proc Natl Acad Sci U S A* (2008) **105**:12051–6. doi:10.1073/pnas.0805953105
27. Dodd MS, Atherton HJ, Carr CA, Stuckey DJ, West JA, Griffin JL, et al. Impaired *in vivo* mitochondrial Krebs cycle activity after myocardial infarction assessed using hyperpolarized magnetic resonance spectroscopy. *Circ Cardiovasc Imaging* (2014) **7**:895–904. doi:10.1161/CIRCIMAGING.114.001857
28. Denton RM, Halestrap AP. Regulation of pyruvate metabolism in mammalian tissues. *Essays Biochem* (1979) **15**:37–77.
29. Gatenby RA, Gillies RJ. Why do cancers have high aerobic glycolysis? *Nat Rev Cancer* (2004) **4**:891–9. doi:10.1038/nrc1478
30. Hanahan D, Weinberg RA. Hallmarks of cancer: the next generation. *Cell* (2011) **144**:646–74. doi:10.1016/j.cell.2011.02.013
31. Golman K, Zandt RI, Lerche M, Pehrson R, Ardenkjaer-Larsen JH. Metabolic imaging by hyperpolarized ^{13}C magnetic resonance imaging for *in vivo* tumor diagnosis. *Cancer Res* (2006) **66**:10855–60. doi:10.1158/0008-5472.CAN-06-2564
32. Park I, Larson PE, Zierhut ML, Hu S, Bok R, Ozawa T, et al. Hyperpolarized ^{13}C magnetic resonance metabolic imaging: application to brain tumors. *Neuro Oncol* (2010) **12**:133–44. doi:10.1093/neuonc/nop043
33. Serrao EM, Kettunen MI, Rodrigues TB, Dzien P, Wright AJ, Gopinathan A, et al. MRI with hyperpolarised [1-^{13}C]pyruvate detects advanced pancreatic preneoplasia prior to invasive disease in a mouse model. *Gut* (2015) **65**(3):465–75. doi:10.1136/gutjnl-2015-310114
34. Hu S, Balakrishnan A, Bok RA, Anderton B, Larson PE, Nelson SJ, et al. ^{13}C-pyruvate imaging reveals alterations in glycolysis that precede c-Myc-induced tumor formation and regression. *Cell Metab* (2011) **14**:131–42. doi:10.1016/j.cmet.2011.04.012
35. Albers MJ, Bok R, Chen AP, Cunningham CH, Zierhut ML, Zhang VY, et al. Hyperpolarized ^{13}C lactate, pyruvate, and alanine: noninvasive biomarkers for prostate cancer detection and grading. *Cancer Res* (2008) **68**:8607–15. doi:10.1158/0008-5472.CAN-08-0749
36. Chen AP, Bok R, Zhang V, Xu D, Veeraraghavan S, Hurd RE, et al. Serial hyperpolarized ^{13}C 3D-MRSI following therapy in a mouse model of prostate cancer. *Proc Int Soc Mag Reson Med* (2008) **16**:888.
37. Krishna MC, Matsumoto S, Saito K, Matsuo M, Mitchell JB, Ardenkjaer-Larsen JH. Magnetic resonance imaging of tumor oxygenation and metabolic profile. *Acta Oncol* (2013) **52**:1248–56. doi:10.3109/0284186X.2013.819118
38. Bluff JE, Reynolds S, Metcalf S, Alizadeh T, Kazan SM, Bucur A, et al. Measurement of the acute metabolic response to hypoxia in rat tumours *in vivo* using magnetic resonance spectroscopy and hyperpolarised pyruvate. *Radiother Oncol* (2015) **116**:392–9. doi:10.1016/j.radonc.2015.03.011
39. Eisenhauer EA, Therasse P, Bogaerts J, Schwartz LH, Sargent D, Ford R, et al. New response evaluation criteria in solid tumours: revised RECIST guideline (version 1.1). *Eur J Cancer* (2009) **45**:228–47. doi:10.1016/j.ejca.2008.10.026
40. Brindle K. New approaches for imaging tumour responses to treatment. *Nat Rev Cancer* (2008) **8**:94–107.1. doi:10.1038/nrc2289
41. Bohndiek SE, Kettunen MI, Hu DE, Brindle KM. Hyperpolarized ^{13}C spectroscopy detects early changes in tumor vasculature and metabolism after VEGF neutralization. *Cancer Res* (2012) **72**:854–64. doi:10.1158/0008-5472.CAN-11-2795
42. Witney TH, Kettunen MI, Hu DE, Gallagher FA, Bohndiek SE, Napolitano R, et al. Detecting treatment response in a model of human breast adenocarcinoma using hyperpolarised [1-^{13}C]pyruvate and [1,4-$^{13}C_2$] fumarate. *Br J Cancer* (2010) **103**:1400–6. doi:10.1038/sj.bjc.6605945
43. Bohndiek SE, Kettunen MI, Hu DE, Witney TH, Kennedy BW, Gallagher FA, et al. Detection of tumor response to a vascular disrupting agent by hyperpolarized ^{13}C magnetic resonance spectroscopy. *Mol Cancer Ther* (2010) **9**:3278–88. doi:10.1158/1535-7163.MCT-10-0706
44. Dafni H, Larson PE, Hu S, Yoshihara HA, Ward CS, Venkatesh HS, et al. Hyperpolarized ^{13}C spectroscopic imaging informs on hypoxia-inducible factor-1 and myc activity downstream of platelet-derived growth factor receptor. *Cancer Res* (2010) **70**:7400–10. doi:10.1158/0008-5472.CAN-10-0883
45. Ward CS, Venkatesh HS, Chaumeil MM, Brandes AH, Vancriekinge M, Dafni H, et al. Noninvasive detection of target modulation following phosphatidylinositol 3-kinase inhibition using hyperpolarized ^{13}C magnetic resonance spectroscopy. *Cancer Res* (2010) **70**:1296–305. doi:10.1158/0008-5472.CAN-09-2251
46. Day SE, Kettunen MI, Cherukuri MK, Mitchell JB, Lizak MJ, Morris HD, et al. Detecting response of rat C6 glioma tumors to radiotherapy using hyperpolarized [1-^{13}C]pyruvate and ^{13}C magnetic resonance spectroscopic imaging. *Magn Reson Med* (2011) **65**:557–63. doi:10.1002/mrm.22698
47. Saito K, Matsumoto S, Takakusagi Y, Matsuo M, Morris HD, Lizak MJ, et al. ^{13}C-MR spectroscopic imaging with hyperpolarized [1-^{13}C]pyruvate detects early response to radiotherapy in SCC tumors and HT-29 tumors. *Clin Cancer Res* (2015) **21**(22):5073–81. doi:10.1158/1078-0432.ccr-14-1717
48. Thind K, Chen A, Friesen-Waldner L, Ouriadov A, Scholl TJ, Fox M, et al. Detection of radiation-induced lung injury using hyperpolarized ^{13}C magnetic resonance spectroscopy and imaging. *Magn Reson Med* (2013) **70**:601–9. doi:10.1002/mrm.24525
49. Thind K, Jensen MD, Hegarty E, Chen AP, Lim H, Martinez-Santiesteban F, et al. Mapping metabolic changes associated with early radiation induced lung injury post conformal radiotherapy using hyperpolarized ^{13}C-pyruvate magnetic resonance spectroscopic imaging. *Radiother Oncol* (2014) **110**:317–22. doi:10.1016/j.radonc.2013.11.016
50. Menzel MI, Farrell EV, Janich MA, Khegai O, Wiesinger F, Nekolla S, et al. Multimodal assessment of *in vivo* metabolism with hyperpolarized [1-^{13}C]MR spectroscopy and ^{18}F-FDG PET imaging in hepatocellular carcinoma tumor-bearing rats. *J Nucl Med* (2013) **54**:1113–9. doi:10.2967/jnumed.112.110825
51. Witney TH, Kettunen MI, Day SE, Hu D, Neves AA, Gallagher FA, et al. A comparison between radiolabeled fluorodeoxyglucose uptake and hyperpolarized ^{13}C-labeled pyruvate utilization as methods for detecting tumor response to Treatment12. *Neoplasia* (2009) **11**:574–82. doi:10.1593/neo.09254
52. Horska A, Barker PB. Imaging of brain tumors: MR spectroscopy and metabolic imaging. *Neuroimaging Clin N Am* (2010) **20**:293–310.1. doi:10.1016/j.nic.2010.04.003
53. Choi C, Ganji SK, Deberardinis RJ, Hatanpaa KJ, Rakheja D, Kovacs Z, et al. 2-hydroxyglutarate detection by magnetic resonance spectroscopy in IDH-mutated patients with gliomas. *Nat Med* (2012) **18**:624–9. doi:10.1038/nm.2682
54. Johnson LM, Turkbey B, Figg WD, Choyke PL. Multiparametric MRI in prostate cancer management. *Nat Rev Clin Oncol* (2014) **11**:346–53. doi:10.1038/nrclinonc.2014.69
55. von Morze C, Larson PE, Hu S, Yoshihara HA, Bok RA, Goga A, et al. Investigating tumor perfusion and metabolism using multiple hyperpolarized ^{13}C compounds: HP001, pyruvate and urea. *Magn Reson Imaging* (2012) **30**:305–11. doi:10.1016/j.mri.2011.09.026
56. Rosenkrantz AB, Friedman K, Chandarana H, Melsaether A, Moy L, Ding YS, et al. Current status of hybrid PET/MRI in oncologic imaging. *AJR Am J Roentgenol* (2016) **206**(1):162–72. doi:10.2214/ajr.15.14968
57. Hensley CT, Wasti AT, Deberardinis RJ. Glutamine and cancer: cell biology, physiology, and clinical opportunities. *J Clin Invest* (2013) **123**:3678–84. doi:10.1172/JCI69600
58. Hosios AM, Vander Heiden MG. Acetate metabolism in cancer cells. *Cancer Metab* (2014) **2**:27. doi:10.1186/s40170-014-0027-y
59. Grassi I, Nanni C, Allegri V, Morigi JJ, Montini GC, Castellucci P, et al. The clinical use of PET with ^{11}C-acetate. *Am J Nucl Med Mol Imaging* (2012) **2**:33–47.
60. Venneti S, Dunphy MP, Zhang H, Pitter KL, Zanzonico P, Campos C, et al. Glutamine-based PET imaging facilitates enhanced metabolic evaluation of gliomas *in vivo*. *Sci Transl Med* (2015) **7**:274ra217. doi:10.1126/scitranslmed.aaa1009
61. Bastiaansen JA, Cheng T, Mishkovsky M, Duarte JM, Comment A, Gruetter R. *In vivo* enzymatic activity of acetylCoA synthetase in skeletal muscle revealed

by ^{13}C turnover from hyperpolarized [1-^{13}C]acetate to [1-^{13}C]acetylcarnitine. *Biochim Biophys Acta* (2013) **1830**:4171–8. doi:10.1016/j.bbagen.2013.03.023
62. Lewis DY, Boren J, Shaw GL, Bielik R, Ramos-Montoya A, Larkin TJ, et al. Late imaging with [1-^{11}C]acetate improves detection of tumor fatty acid synthesis with PET. *J Nucl Med* (2014) **55**:1144–9. doi:10.2967/jnumed.113.134437
63. Gallagher FA, Kettunen MI, Day SE, Lerche M, Brindle KM. ^{13}C MR spectroscopy measurements of glutaminase activity in human hepatocellular carcinoma cells using hyperpolarized ^{13}C-labeled glutamine. *Magn Reson Med* (2008) **60**:253–7. doi:10.1002/mrm.21650
64. Cabella C, Karlsson M, Canape C, Catanzaro G, Colombo Serra S, Miragoli L, et al. *In vivo* and *in vitro* liver cancer metabolism observed with hyperpolarized [5-^{13}C] glutamine. *J Magn Reson* (2013) **232**:45–52.1. doi:10.1016/j.jmr.2013.04.010
65. Radon TP, Massat NJ, Jones R, Alrawashdeh W, Dumartin L, Ennis D, et al. Identification of a three-biomarker panel in urine for early detection of pancreatic adenocarcinoma. *Clin Cancer Res* (2015) **21**:3512–21. doi:10.1158/1078-0432.CCR-14-2467
66. Murtaza M, Dawson SJ, Tsui DW, Gale D, Forshew T, Piskorz AM, et al. Non-invasive analysis of acquired resistance to cancer therapy by sequencing of plasma DNA. *Nature* (2013) **497**:108–12. doi:10.1038/nature12065
67. Bettegowda C, Sausen M, Leary RJ, Kinde I, Wang Y, Agrawal N, et al. Detection of circulating tumor DNA in early- and late-stage human malignancies. *Sci Transl Med* (2014) **6**:224ra224. doi:10.1126/scitranslmed.3007094

Conflict of Interest Statement: KB's lab has a research agreement with GE Healthcare (GEH) and holds patents on DNP technology with GEH.